Conference Paper, Published Version

Gonzalez Duenas, Catalina; Bernier, Carl; Padgett, Jamie

Probabilistic Assessment of Bridges Subjected to Waterborne Debris

Coastal Structures 2019 - Nils Goseberg, Torsten Schlurmann (eds) - © 2019 Bundesanstalt für Wasserbau
ISBN 978-3-939230-64-9 (Online) - DOI: 10.18451/978-3-939230-64-9_036

Probabilistic Assessment of Bridges Subjected to Waterborne Debris

C. Gonzalez Duenas, C. Bernier & J. E. Padgett
Rice University, Houston, United States

Abstract: Waterborne debris during storm surge events can impose significant impact loads and thereby cause severe damage to coastal structures. While several studies have characterized debris impact loads, very few studies have actually focused on the structural behavior and vulnerability of coastal structures, like bridges, subjected to such impacts. This study investigates the structural response of a case study bridge subjected to water-driven debris impacts and develops its associated fragility model during storm surge events. First, the hydrodynamic conditions at the bridge location are defined. Next, finite element models of the debris and a typical pier system of the case study bridge are developed and validated to compute the demands imposed on a column by the impact of the debris. An analysis of variance (ANOVA) is then conducted to study the influence of different parameters on the imposed demands. Finally, a statistical sampling method and logistic regression are used to derive a fragility model and assess the vulnerability of the case study bridge. The resulting fragility models can be used for rapid vulnerability assessment, evaluation of mitigation strategies, and to obtain key insights concerning the effects of each parameter on the probability of shear failure of a bridge column under debris impact.

Keywords: Debris; Bridges; Hurricanes; Impact loads; Fragility; Sensitivity analysis; Finite element model.

1 Introduction

Waterborne debris during storm surge events can impose significant impact loads and thereby cause severe damage to coastal structures like bridges. These loads can lead not only to severe local structural damage but also to progressive collapse due to loss of support of the structure (Deng, Wang and Yu, 2016). For instance, during Hurricane Katrina different types of debris, including a barge and tug boat, impacted the eastbound I-10 Pascagoula River Bridge, leading to significant structural damage of piles, fascia girders and large transverse displacement (Padgett et al., 2008). Hence, proper characterization of the demands imposed on the impacted structural components is of vital importance for the design and vulnerability assessment of coastal infrastructure. Previous studies have focused on the impact loads caused by massive objects such as vessel (Davidson, 2010; Davidson and Getter, 2010; Fan et al., 2011; Wang and Wang, 2015) and barge (Wardhana and Hadipriono, 2003; Davidson, 2010) collisions on bridges. However, more recently attention has been paid to the impact loads generated by shipping containers due to their broad presence in hurricane and tsunami-prone regions (Madurapperuma and Wijeyewickrema, 2013; Aghl et al., 2014; Aghl, Naito and Riggs, 2015a, 2015b).

Current design code (AASHTO, 2014) only considers vessel and barge collisions for bridge design purposes (Manuel et al., 2006). In the code, the risk of collapse of the bridge is evaluated using an empirical expression of the annual frequency of collapse. This expression was formulated based on a study of ship-to-ship collisions (Cowiconsult, 1987; Davidson and Consolazio, 2010). In an effort to consider barge impact scenarios in the probability of collapse, Davidson and Consolazio (2010) developed a revised probability of collapse expression for bridges subjected to such impact. In their study, the probability that the bridge will collapse under barge collision was evaluated by varying different input parameters in each analysis that lead to different realizations of both the impact forces and the strengths of the bridge. However, the consideration of other types of collision events, such as the impact of debris, is still missing in the AASHTO code. On the other hand, ASCE/SEI 7-16 (ASCE/SEI, 2016) requires the estimation of debris impact loads in regions where inundation depths are expected to exceed the specified minimum inundation depth (0.914 m). In particular, the site hazard assessment for shipping containers requires the calculation of a probable dispersion region prior to the evaluation of the impact force from the shipping container and the duration of the impact.

In recent years, the characterization of the impact loads generated by shipping containers, as well as the duration of the impact has been a focus of study. Aghl et al. (2015b) conducted an experimental study to quantify the impact forces and durations from three different debris types: a full-scale wood utility pole, a 6.1 m steel tube and a standard International Organization for Standardization (ISO) shipping container. The results of the experiments were then used to validate a one-dimensional elastic impact model for the estimation of the peak impact force and duration. Ko et al. (2015) conducted hydraulic experiments on the impact loads generated on a column by the collision of a 1:5 scaled shipping container. The authors found that the hydrodynamic effects showed an increase in the impact load duration compared to in-air tests and that the non-structural mass had a significant influence on the overall impulse on the column. To study the effect of nonstructural mass on debris impact demands, Aghl et al. (2015a) developed full-scale experiments and nonlinear finite element models on an empty and three different configurations of loaded shipping containers. Their results indicated that the inelastic response of the container limits the impact force at elevated impact velocities. A one-dimensional model was proposed to evaluate the peak impact force and duration generated from debris impact. However, the structural behavior and vulnerability of the structures subjected to the debris impact loads were not addressed in the above-mentioned studies. To overcome this drawback, Madurapperuma and Wijeyewickrema (2013) evaluated the response of two types of reinforced concrete (i.e. square and circular cross-section) columns under the impact of 20-ft (6.1 m) and 40-ft (12.2 m) ISO shipping containers. Finite element models for the 20-ft and 40-ft containers were developed and different container-column impact configurations for the square and circular cross-sectional columns were examined. In the analyses, columns exhibited severe local deformation followed by shear failure and subsequent loss of axial load carrying capacity. It was observed that the peak impact force imparted on the column was influenced by both the impact configuration and the cross-section of the column. The damage of the impacted column was evaluated with the use of a damage index, which represented the loss of the axial load carrying capacity of the column. So far, the probability of failure of the columns was not explicitly addressed. In this regard, Karafagka et al. (2018) developed analytical fragility curves which yield a probability of failure of columns as a function of inundation depth for a steel frame warehouse as well as different types of RC buildings subjected to tsunami forces. In the study, the waterborne debris impact force was computed as a static load using the FEMA P-646 equation (FEMA, 2012). The type of debris considered for the analysis was a lumber of wood. Thus, previous studies revealed the lack of adequate emphasis on the characterization of the structural response of bridges under debris impact load and subsequent computation of its probability of failure.

This study aims to evaluate the structural behavior of a case study bridge subjected to water-driven debris impacts and develop fragility models to efficiently assess the vulnerability of the case study bridge to debris impacts during storm surge events. First, the numerical modeling of the debris and a typical pier system of the case study bridge is developed to compute the demands imposed on a column by the impact of a shipping container. The mode of failure consider herein is shear failure. An analysis of variance (ANOVA) is then conducted to study the influence of different modeling parameters on the imposed demands. Next, a statistical sampling method and logistic regression are used to derive fragility models for three performance levels and assess the vulnerability of the case study bridge. Finally, the effects of debris impact load on the structural performance and the probability of shear failure of the case study bridge column are discussed.

2 Numerical Modeling of Impact Loads on the Bridge Column

Adequate estimation of the imposed demand on the case study bridge is first required to characterize the structural response of the column subjected to debris impact and to develop fragility models. The case study bridge considered in this paper for illustrating a method to derive impact fragility models corresponds to a typical multi-span simply supported (MSSS) concrete girder bridge located in the Houston-Galveston area (Fig. 1). Due to the broad observed presence of shipping containers in storm and tsunami-prone regions, a standard 20-ft ISO shipping container is selected as the impact object for the study. *LS-Dyna* (LSTC, 2015) is used to model the shipping container and a pier system of one of the main spans of the case study bridge. The pier system consists of two circular columns with a total height of 15.24 m connected by a 3 m-height stiffening beam at a height of 10.21 m from the ground. The columns have a diameter of 0.91 m below the stiffening beam and a diameter of 0.76 m on top of it.

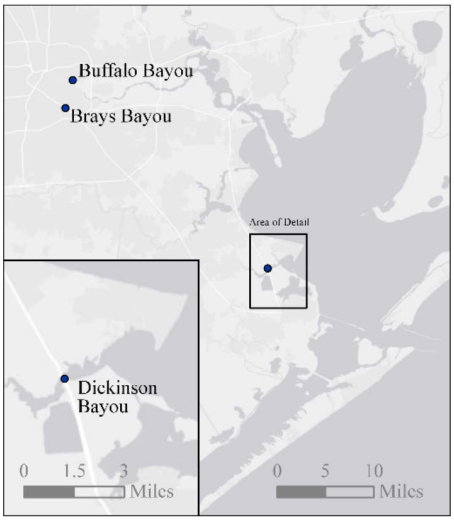

Fig. 1. Location of the case study bridge in the Houston-Galveston area

The pier model consists of 333,921 nodes and 304,370 fully integrated S/R solid elements, with a constant mesh size of 0.05 m. Displacement and rotation degrees of freedom at the base of the columns are restrained (El-Tawil et al., 2005; Thilakarathna et al., 2010). The self-contact of the pier elements is modeled using a TIED_NODES_TO_SURFACE CONTACT TYPE. The loads imposed by the two adjacent spans are placed as a uniform pressure on the top of the bent beam. As a first approximation to the problem, an elastic concrete material model is selected for the pier. It is acknowledged that relatively higher values of base shear will be estimated as opposed to a material that allows damage; however, in this study, this method is assumed to be conservative and future work will address this limitation. The 20-ft ISO shipping container has overall dimensions of 6.1 m long, 2.4 m wide and 2.6 m high, and has a tare mass of 2100 kg. The model consists of 36.387 nodes and 37,410 elements. The material MAT_PLASTIC_KINEMATIC is used for the shipping container with the following properties: 7800 kg/m^3 for the steel mass density, Young's modulus of 207 GPa, a Poisson's ratio of 0.3, yield stress of 380 MPa, a tangent modulus of 1000 MPa and a failure strain of 25%. The shipping container model is validated against experimental results from a series of full-scale in-air shipping container impacts tests (Piran Aghl et al., 2014; Bernier and Padgett, 2019). Further details of the modeling and design considerations are given in Bernier (2019). The contact between the pier and the shipping container is defined as an AUTOMATIC_SURFACE_TO_SURFACE contact type with a static coefficient of friction of 0.65 (Jrabbat and Russell, 1985). Fig. 2 shows the FE models of the bridge pier and the shipping container.

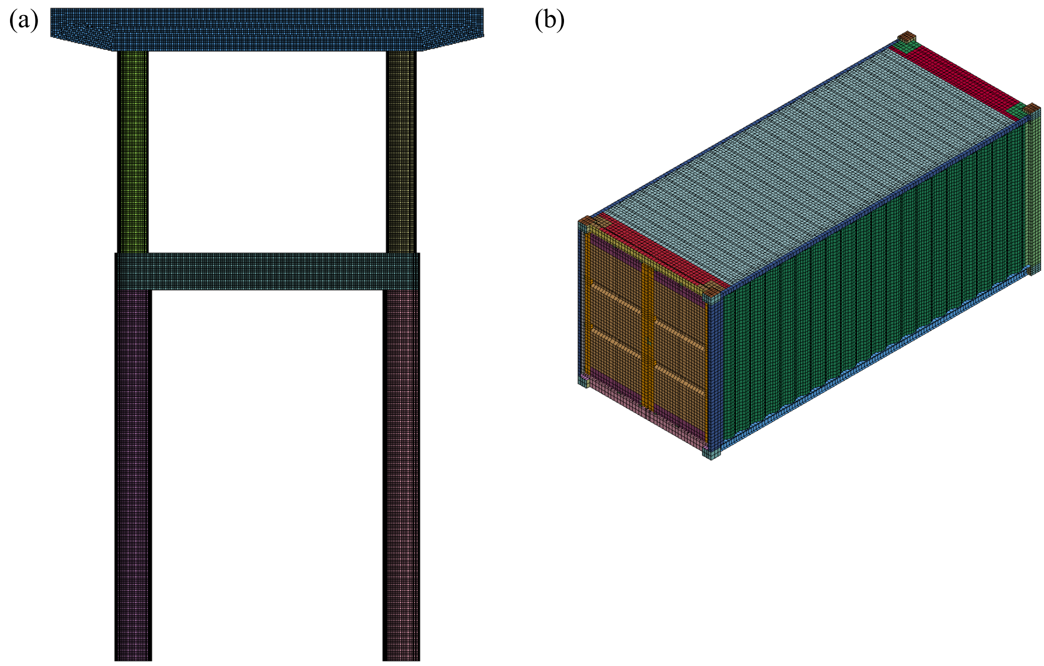

Fig. 2. LS-Dyna models of (a) pier system, (b) shipping container.

3 Sensitivity Analysis

An analysis of variance (ANOVA) is conducted to study the influence of different modeling parameters on the structural response of the column under the impact of the shipping container. Based on the work by Madurapperuma and Wijeyewickrema (2013), the engineering demand parameter (EDP) selected in the current study is the shear force on the base of the impacted columns. The null hypothesis implied in the ANOVA states that the mean values of the considered factors are equal, and the alternative hypothesis affirms that at least one of the mean values is different, and thus, relevant for the analysis (Walpole et al., 2012). A level of significance of 5% is adopted for the acceptance of the null hypothesis, hence, a *p*-value higher than this level implies the rejection of the alternative hypothesis. The selected factors for the analyses are (1) the surge height at the bridge location; (2) the concrete strength of the pier; (3) the impact configuration (Fig. 3); (4) the mass and (5) the initial velocity of the container.

The hydrodynamic conditions considered at the bridge location are based on two synthetic storms developed by the Federal Emergency Management Agency (FEMA), which produce water elevations corresponding to return periods of 100 and 500 years at the bridge location (FEMA, 2013). The surge heights considered in the analyses (5.12 m for the lower bound and 5.54 m for the upper bound, with respect to the bottom of the column) are then used to calculate the draft of the container and the respective impact heights for the FE analyses. The container impact velocities are calculated based on the FEMA (2011) design flood velocity equations, which provide a lower and an upper bound of flood velocity in coastal areas based on the design stillwater flood depth. The levels considered for the velocity factor correspond to (1) the upper bound of the 5.12 m flood depth, and to the (2) lower and (3) upper bounds of the 5.54 m flood depth. For the mass factor, two levels are chosen: (1) mass of the empty container (2100 kg), and (2) total mass considering both the mass of the empty container and a nonstructural mass of 2200 kg. The latter value is obtained from Madurapperuma and Wijeyewickrema (2013). To evaluate the influence of the material properties in the model, a normal distribution with a *cov* of 0.17 and a mean value of 25.29 MPa is adopted for the compressive strength of concrete (Ellingwood and Hwang, 1985; Ataei, 2013). Three different levels are considered for this factor, corresponding to the mean value, and the mean value plus and minus one standard deviation. The impact configurations correspond to the L3, T1 and C1 configurations in Madurapperuma and Wijeyewickrema (2013). These configurations were found by the authors to have the most significant influence in the peak impact load for circular columns (Fig. 3). Table 1 summarizes the proposed statistical experimental design.

Tab. 1. Statistical experimental design

Factor	Level 1	Level 2	Level 3
Velocity*, m/s	5.54	7.09	7.37
Mass, kg	2100	4300	-
Surge height, m	5.12	5.54	-
Compressive strength of concrete, MPa	25.29	20.99	29.59
Impact Configuration	L3	T1	C1

* Blocking parameter.

The statistical software STATA (StataCorp, 2015) is used to conduct the sensitivity study. As the current study is based on numerical simulations, just one experimental unit was considered in each treatment. Table 2 shows the results of the analysis of variance, where a *p*-value less than 5% indicates the significance of the factor in the model.

Tab. 2. *p*-value results for the analysis of variance (ANOVA)

Factor	*p*-value
Velocity, m/s	0.001*
Mass, kg	0.001*
Surge height, m	0.000*
Compressive strength of concrete, MPa	0.1
Impact Configuration	0.000*

* *p*-value less than 0.05

The ANOVA results show that the concrete strength of the pier does not have an influence on the shear demand generated at the base of the column. However, the surge height, the impact configuration, the velocity and the mass of the container show a significant effect on the shear demand. Hence, these factors are used as significant parameters in the fragility model proposed in Section 4.

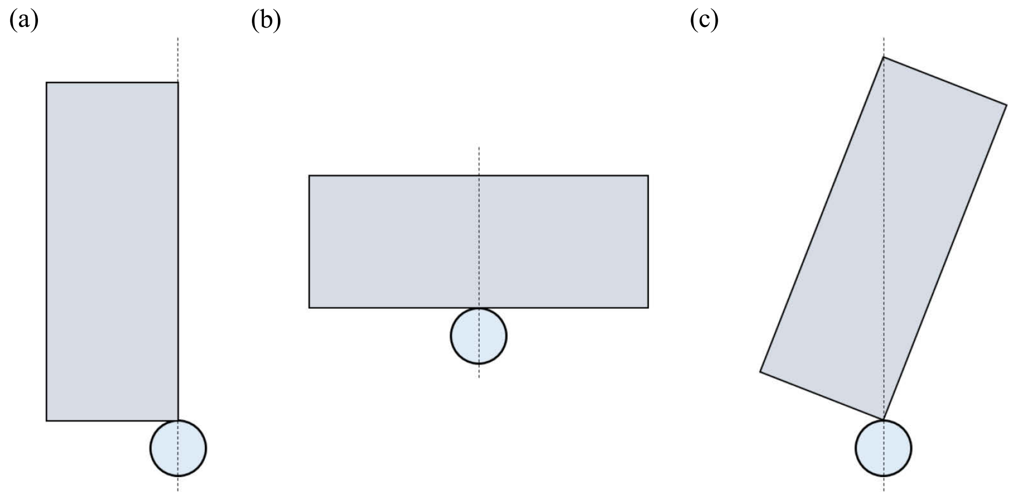

Fig. 3. Plan-view of the (a) L3, (b) T1, and (c) C1, impact configurations.

4 Fragility Analysis

In this study, a parameterized model is proposed to evaluate the fragility of the bridge under debris impact. The parameterized fragility model provides the probability of exceeding certain limit states of the structure as a function of an intensity measure of the hazard. To characterize the fragility of the system, a limit state function is defined as:

$$g_{PL} = C_{PL} - D \quad (1)$$

where g_{PL}= limit state function for a given performance level, C_{PL}= capacity of the column for a given performance level, and D = demand imposed on the column by the impact of the shipping container. The system is considered to have failed when the limit state equation is below zero.

4.1 Probabilistic demand model

A Latin Hypercube Sampling (LHS) method is used to span the set of influencing debris impact parameter values required for the experimental design (McKay et al., 1972). Table 3 summarizes the ranges of the debris impact conditions considered in the analysis for the continuous variables. For exploration purposes, the range of the surge height is rounded off to the nearest integer based on the range of hydrodynamic conditions discussed in the previous section. For the impact configuration (*IC*), a uniform probability distribution is assumed by assigning a probability of 1/3 to each configuration. The lower and upper bounds for the mass of the container correspond to 2100 kg (an empty container) and to the maximum gross weight of the shipping container (30,400 kg), respectively. The initial velocity of the container is treated here as a dependent variable which varies as a function of the surge height. Therefore, for each sampled value of surge height, the range of the velocity of the container is computed using the lower and upper bounds of the FEMA (2011) design flood velocity equation. A total of 200 samples were generated using LHS, each one representing a specific debris impact condition.

Tab. 3. Ranges of debris impact conditions for continuous variables

Parameter	Lower bound	Upper bound	Units
Surge height (*S*)	5.00	6.00	m
Mass (*M*)	2100	30,400	kg
Debris velocity (*V*)	5.11	7.59	m

4.2 Probabilistic capacity model

The probabilistic shear capacity model developed by Sharma et al. (2015) is used in this study to estimate the capacity of the column under the impact of the shipping container. The authors proposed capacity models for reinforced concrete (RC) columns under vehicle collision for three different performance levels: (1) fully operational with no damage (P1); (2) operational structure with damage (P2); (3) collapse prevention (P3). These performance levels are associated with four damage levels (DL) that the column can experience due to the collision. With an increasing intensity of 1 to 4, these damage levels correspond to: (1) insignificant damage (D1); (2) minor spalling of concrete, yielding of longitudinal steel (D2); (3) significant cracking of concrete, spiral and longitudinal bar exposed, buckling of bars (D3); and (4) loss of axial load capacity, longitudinal bar fracture (D4) (Sharma, Gardoni and Hurlebaus, 2015). Performance levels P1, P2, and P3 are defined as the maximum shear capacity before D2, D3 and D4 start occurring, respectively. The authors proposed a probabilistic model of shear capacity for each of the performance levels by incorporating correction terms with previously existing deterministic mechanical models, whose general form is shown in Eq. (2).

$$\ln[v_{Pi}(x, \theta_{Pi})] = \ln[\hat{v}_{Pi}(x)] - \gamma_{Pi}(x, \theta_{Pi}) + \sigma_{Pi}e_{Pi} \quad (2a)$$

where $v_{Pi} = V_{Pi}/NF_{Pi}$ = normalized dynamic shear force capacity for performance levels P_i; V_{Pi} = dynamic shear force capacity; NF_{Pi} = normalizing factor for dynamic shear force capacity to produce a dimensionless quantity; $\hat{v}_{Pi}(x)$ = normalized dynamic shear force capacity obtained from mechanical model $\hat{V}_{Pi}$, $\gamma_{Pi}(x, \theta_{Pi})$ = correction term for the bias inherent mechanical model defined as

$$\gamma_{Pi}(x, \theta_{Pi}) = \sum_{j=1}^{k_{Pi}} \theta_{Pi,j} h_{Pi,j}(x) \quad (2b)$$

where $h_{Pi,j}(x), j = 1, \ldots, k$ = explanatory function defined as function of X, $\theta_{Pi,j}(x), j = 1, \ldots, k_{Pi}$, are the parameters associated with the explanatory functions, $\sigma_{Pi}e_{Pi}$ = model error with zero mean and unit variance, e_{Pi} = random variable with zero mean and unit variance, σ_{Pi} = standard deviation of the model error (Gardoni et al., 2002; Sharma et al., 2015). An exhaustive experimental design was conducted using FE models by varying the parameters of the column as well as the vehicle within a realistic range. The coefficients, $\theta_{Pi,j}$, of the proposed probabilistic models were obtained using the Bayesian model updating framework with the results of each numerical simulation. The framework yielded the mean vector and the covariance matrix of the coefficients, which incorporated model uncertainty. The probabilistic model proposed by Sharma et al. (2015) is, to the knowledge of the authors, the most adaptable to the current case study, since it considers: (1) the dependency of the structure capacity on the nature of the collision event (i.e. velocity and mass of the vehicle, relative stiffness of the bodies), (2) the influence of the dynamic shear action on the capacity of the column for large mass and high velocity impacting vehicles, and (3) different performance levels for the estimation of the column shear capacity (Sharma, Gardoni and Hurlebaus, 2015). It is also noteworthy, that the range of the parameters used in this study for the structural characterization of the columns, as well as the intensity of the impact scenarios (mass and velocity of the container), coincides with the range of the parameters considered by Sharma et al. (2015) in the FE simulations and experimental design.

4.3 Fragility model

For each of the 200 parameter combinations of the LHS sample, 10,000 instances of shear capacity values are generated using the probabilistic model discussed in the previous section. Such a large number of shear capacity instances for a particular LHS sample is generated in order to obtain a reasonably good approximation of the distribution of the exact shear capacity. The probability of failure for the three performance levels is then computed using the shear demand for the corresponding LHS sample and evaluating the limit state function (Eq. (1)). The ratio of the number of instances of shear capacity falling short of the shear demand, to the total number of generated shear capacity instances (10,000), represents the probability of failure for a specific LHS sample. The process is repeated for each LHS demand combination (200 samples varying *S*, *M*, *V*, and *IC*). In order to obtain failure probability as a mathematical function of the selected parameters used for generating LHS samples, the probability of failure is modeled as a logit function with *S*, *M*, *V*, and *IC* as its parameters as given by Eq. (3). The coefficients of the model are computed using 80% of the data as the training set. The obtained coefficients of the three performance level models are reported in Eq. (4).

$$P(\text{Failure}|S,M,V,IC) = \frac{1}{1+\exp(-l(S,M,V,IC))} \tag{3}$$

where $l(\cdot)$ is a linear function given by Eq. (4) for the considered performance levels. The accuracy of each model is evaluated using the 20% remaining data labeled as the test set. Both the predicted outcome as well as true outcome are converted to a binary response by setting a hard threshold of 50%, which means the outcome is 0 if the probability of failure is less than the threshold, else 1. The obtained accuracy on the test samples, for the models, are 100 %, 90%, and 100% respectively for the three performance levels P1, P2, and P3.

$$l(S,M,V,IC)_{P1} = 1.78 - 0.07S + 0.00013M + 0.085\,V + 0.012IC \tag{4a}$$

$$l(S,M,V,IC)_{P2} = -2.10 + 0.10S + 0.000035M + 0.23\,V + 0.057IC \tag{4b}$$

$$l(S,M,V,IC)_{P3} = -12.56 - 0.10S + 0.00012M + 0.70\,V + 0.23IC \tag{4b}$$

The fragility models for the performance levels P1, P2, and P3 as a function of the total mass of the container (*M*) are presented in Fig. (4) for three different impact configurations. To generate the one-dimensional fragility curve, the initial velocity of the container V and the surge height S, are set constant with values of 6.35 m/s and 5.5 m respectively. For the three performance levels, Fig. (4) shows that as the mass of the container increases, the probability of failure also increases. On the other hand, the impact configuration shows a significant effect on performance levels 2 and 3, and a reduced effect on performance level 1. Impact configuration 3 produces the highest value of failure probability, followed by impact configuration 2 and then 1. For the performance levels P1, P2 and P3, Fig. (5) shows the fragility models as a function of the initial velocity of the container. For all three performance levels, as the velocity of the container increases higher values of probability of failure are obtained. An increment in the probability of failure is also observed for impact configuration 3 compared to configurations 2 and 1.

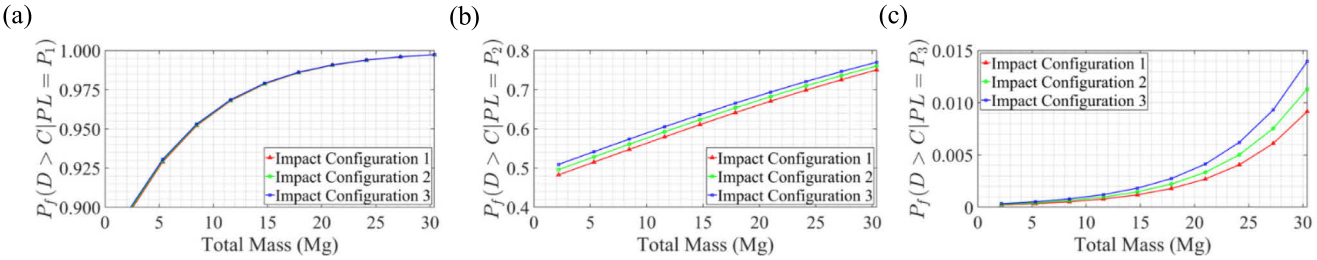

Fig. 4. Debris impact fragility curves for performance levels (a) P1, (b) P2, and (c) P3; with $V = 6.35$ m/s and $S = 5.5$ m.

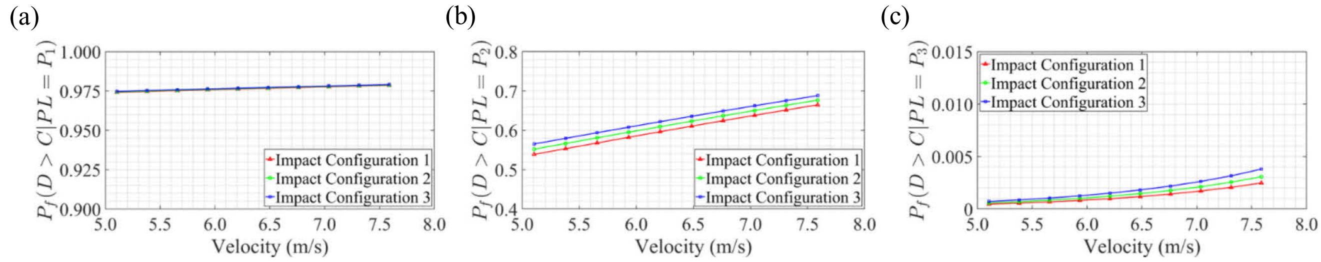

Fig. 5. Debris impact fragility curves for performance levels (a) P1, (b) P2, and (c) P3; with $M = 14$ Mg and $S = 5.5$ m.

The increase in the probability of failure with increasing mass and velocity is expected since these two variables are directly related with the energy transmitted to the column by the impact of the shipping container and the duration of the impact. For impact configuration 3, stiff structural components of the shipping container resist its deformation during the impact, increasing the transferred energy to the column, and thus, leading to higher probabilities of failure. In the case of impact configuration 1, even though stiff components resist the deformation of the container, rotation is more likely to occur reducing the transmission of the energy (Madurapperuma and Wijeyewickrema, 2013). The relatively low probability of failure for the performance level 3 is expected for the range of debris impact parameters considered in the study. If larger values of debris impact conditions (*S*, *M*, *V,* and *IC*) are considered, an increase in the probability of failure associated with the performance level 3 would be expected. From the results of the analysis, it can be inferred that it is highly probable that the performance level 1 will be exceeded whereas it is much less probable for performance level 3 to be exceeded. The obtained fragility functions for all three performance levels can be used to compute the probability of failure of the column of the bridge considered in the present study for any combination of the four most sensitive parameters reported in Section 3.

5 Conclusions

In this study, existing gaps in the characterization of the structural response of bridges under debris impact load and the computation of its probability of failure are addressed. A case study bridge is used to illustrate a framework for the evaluation of the probability of failure of a column subjected to the impact of a standard 20-ft ISO shipping container during storm-surge events. The mode of failure considered was shear failure. First, finite element (FE) models of the debris and a typical pier system of the case study bridge were developed to compute the demands imposed on a column by the impact of the shipping container. The hydrodynamic conditions at the bridge location were defined using numerical simulations of synthetic storms in and around the Houston-Galveston area. Next, an analysis of variance (ANOVA) was conducted to identify the most important parameters on the imposed shear demand. Results showed that the initial velocity and mass of the container, impact configuration and surge height have and influence on the shear force demand generated at the base of the column. Finally, a statistical sampling method and logistic regression were used to derive fragility models for three performance levels and assess the vulnerability of the case study bridge. The results indicated that the velocity and the mass of the shipping container had the strongest effect on the increase of the probability of failure of the column. The fragility models proposed can now be used for rapid vulnerability assessment and evaluation of mitigation strategies under a range of reasonable debris impact conditions for the bridge study case. These models also provided key insights regarding the probability of exceeding three different performance levels. Results indicated that there is a high likelihood of exceeding the performance level 1, whereas the performance level 3 has significant low values of probability of exceedance for the study case considered. As a first effort to characterize the fragility of bridges subjected to debris impact, this study will open the path for future research studies considering other types of debris, regional risk assessment and evaluation of a portfolio of bridges. Future work should also address additional complexities, such as the consideration of material nonlinearities in the FE models, system level response and vulnerability modeling of bridges subjected to debris, and the uncertainties associated with the structural and material characteristics in the fragility models.

6 Acknowledgement

The authors acknowledge the financial support of the National Science Foundation under the PIRE program. Any opinions, findings, and conclusions or recommendations expressed in this paper are those of the authors and do not necessarily reflect the views of the sponsors.

References

AASHTO, 2014. AASHTO LRFD bridge design specifications. Washington, D.C.: American Association of State Highway and Trasnportation Officials.

Aghl, P., Naito, C. J., and Riggs, H. R., 2014. Full-scale experimental study of impact demands resulting from high mass, low velocity debris. Journal of Structural Engineering, 140(5), 04014006.

Aghl, P. P., Naito, C. J., and Riggs, H. R., 2015a. Effect of nonstructural mass on debris impact demands : Experimental and simulation studies. Engineering Structures, Elsevier, 88, 163–175.

Aghl, P.P., Naito, C., and Riggs, H., 2015b. Estimation of demands resulting from inelastic axial impact of steel debris. Engineering Structures, Elsevier, 82 (1), 11–21.

ASCE/SEI, 2016. ASCE/SEI 7-16. Minimum Design Loads and Associated Criteria for Buildings and Other Structures.

Ataei, N., 2013. Vulnerability assessment of coastal bridges subjected to hurricane events, Ph.D. Thesis, Rice University.

Bernier, C., 2019. Fragility and Risk Assessment of Aboveground Storage Tanks during Storm Events, Ph.D. Thesis, Rice University.

Bernier, C., and Padgett, J.E., 2019. Probabilistic assessment of storage tanks subjected to waterborne debris impacts during storm events. Journal of Waterway, Port, Coastal, and Ocean Engineering, in review.

COWIconsult, R. I. A. S., 1987. General principles for risk evaluation of ship collisions, strandings, and contact incidents.

Davidson, M. T., and Consolazio, G. R., 2010. Development of an Improved Probability of Collapse Expression for Bridge Piers Subject to Barge Impact, in Structures Congress 2010, pp. 3321–3332.

Consolazio, G. R., Davidson, M. T., and Getter, D. J., 2010. Vessel crushing and structural collapse relationships for bridge design (No. Report No. 2010/72908/74039). University of Florida, Department of Civil & Coastal Engineering.

Deng, L., Wang, W., and Yu, Y., 2015. State-of-the-art review on the causes and mechanisms of bridge collapse. Journal of Performance of Constructed Facilities, 30(2), 04015005.

Ellingwood, B., and Hwang, H., 1985. Probabilistic descriptions of resistance of safety-related structures in nuclear plants. Nuclear Engineering and Design, 88(2), 169-178

El-tawil, S., Severino, E., and Fonseca, P., 2005. Vehicle Collision with Bridge Piers. Journal of Bridge Engineering, 10(3), 345–353.

Fan, W., Yuan, W., Yang, Z., and Fan, Q., 2010. Dynamic demand of bridge structure subjected to vessel impact using simplified interaction model. Journal of Bridge Engineering, 16(1), 117-126.

Federal Emergency Management Agency, 2011. Coastal Construction Manual.

Federal Emergency Management Agency, 2012. Guidelines for Design of Structures for Vertical Evacuation from Tsunamis.

Federal Emergency Management Agency, 2013. Flood Insurance Study - Harris County, Texas and 559 Incorporated Areas, Preliminary study 48201CV001A. 2013.

Gardoni, P., Der Kiureghian, A., and Mosalam, K. M., 2002. Probabilistic capacity models and fragility estimates for reinforced concrete columns based on experimental observations. Journal of Engineering Mechanics, 128(10), 1024-1038.

Rabbat, B. G., and Russell, H. G, 1985. Friction coefficient of steel on concrete or grout. Journal of Structural Engineering, 111(3), 505-515.

Karafagka, S., Fotopoulou, S., and Pitilakis, K., 2018. Analytical tsunami fragility curves for seaport RC buildings and steel light frame warehouses. Soil Dynamics and Earthquake Engineering, 112, 118-137.

Ko, H. S., Cox, D. T., Riggs, H. R., and Naito, C. J., 2014. Hydraulic experiments on impact forces from tsunami-driven debris. Journal of Waterway, Port, Coastal, and Ocean Engineering, 141(3), 04014043.

Madurapperuma, M. A. K. M., and Wijeyewickrema, A. C., 2013. Response of reinforced concrete columns impacted by tsunami dispersed 20′ and 40′ shipping containers. Engineering Structures, 56, 1631-1644.

Manuel, L., Kallivokas, L. F., Williamson, E. B., Bomba, M., Berlin, K. B., Cryer, A., and Henderson, W. R., 2006. A probabilistic analysis of the frequency of bridge collapses due to vessel impact. No. FHWA/TX-07/0-4650-1.

Padgett, J., DesRoches, R., Nielson, B., Yashinsky, M., Kwon, O. S., Burdette, N., and Tavera, E., 2008. Bridge damage and repair costs from Hurricane Katrina. Journal of Bridge Engineering, 13(1), 6-14.

Piran Aghl, P., Naito, C. J., and Riggs, H. R., 2014. Full-Scale Experimental Study of Impact Demands Resulting from High Mass, Low Velocity Debris. J. of Structural Engineering, 140(5), 04014006.

Sharma, H., Gardoni, P., and Hurlebaus, S., 2015. Performance-based probabilistic capacity models and fragility estimates for RC columns subject to vehicle collision. Computer-Aided Civil and Infrastructure Engineering, 30(7), 555-569.

Thilakarathna, H. M. I., Thambiratnam, D. P., Dhanasekar, M., and Perera, N., 2010. Numerical simulation of axially loaded concrete columns under transverse impact and vulnerability assessment. International Journal of Impact Engineering, 37(11), 1100–1112. https://doi.org/10.1016/j.ijimpeng.2010.06.003.

Walpole, R. E., Myers, R. H., Myers, S. L., and Ye, K., 1993. Probability and statistics for engineers and scientists. Vol. 5. Macmillan; New York.

Wang, J., and Wang, W., 2014. Estimation of Vessel-Bridge Collision Probability for Complex Navigation Channels. Journal of Bridge Engineering, 20(7), 04014091.

Wardhana, K., and Hadipriono, F. C., 2003. Analysis of recent bridge failures in the United States. Journal of performance of constructed facilities, 17(3), 144-150.